J|A|C|S ARTICLES

Published on Web 10/21/2009

Formation of PbS Nanowire Pine Trees Driven by Screw Dislocations

Y. K. Albert Lau, Davin J. Chernak, Matthew J. Bierman, and Song Jin*

Department of Chemistry, University of Wisconsin−Madison, 1101 University Avenue, Madison, Wisconsin 53706

Received August 1, 2009; E-mail: jin@chem.wisc.edu

Abstract: The basic characteristics of nanowire growth driven by screw dislocations were investigated by synthesizing hierarchical lead sulfide (PbS) nanowire "pine trees" using chemical vapor deposition of $PbCl_2$ and S precursors and systematically observing the effects of various growth parameters, such as hydrogen flow, temperature, pressure, and the growth substrates employed. Statistical surveys showed that the growth rate of the dislocation-driven trunk is about 6 μm/min and that of the vapor-liquid-solid (VLS) driven branch nanowire is about 1.2 μm/min under the typical reaction conditions at 600 °C, 900 Torr, and a hydrogen flow rate of 1.5 sccm. The onset of hydrogen flow plus the presence of fresh silicon have been identified as the critical ingredients for generating PbS nanowire trees reproducibly. To explain the experimental findings in the context of classical crystal growth theory, the former is suggested to create a spike in supersaturation of the actual sulfur precursor H_2S and initiate dislocations with screw components that then propagate anisotropically to form the PbS nanowire trunks. Maintaining suitable hydrogen flow provides a favorable low supersaturation that promotes dislocation-driven trunk nanowire growth and enables the simultaneous VLS nanowire growth of branches. Furthermore, thermodynamic consideration and experiments showed that silicon fortuitously controls the supersaturation by reversibly reacting with H_2S to form SiS_2 and that SiS_2 can also be a viable precursor for PbS nanowire growth. The key requirements of screw dislocation-driven nanowire growth are summarized. This study provides some general guidelines for further nanowire growth driven by screw dislocations.

1. Introduction

One-dimensional (1-D) nanomaterials such as nanowires, nanobelts, and nanotubes possess novel properties that have already found many applications in nanoelectronics, nanophotonics, renewable energy, and chemical and biological sensing.[1−8] So far, the well-known vapor-liquid-solid (VLS) mechanism has been the most commonly discussed mechanism for bottom-up synthesis of nanowires.[9,10] In the VLS mechanism, a nanocatalyst (e.g., Au) is supersaturated with the desired gaseous species (e.g., Si) to form a liquid droplet due to eutectic phase behavior, which leads to the precipitation of the nanowire material (e.g., Si). 1-D growth is driven by the liquid-solid interface, while the diameter of nanowire is determined by the catalyst size. Analogous mechanisms such as solution-liquid-solid[11,12] and vapor-solid-solid[13] growth have also been used to synthesize nanowires. In the 1950s, before VLS growth was discovered, Sears had proposed that axial screw dislocations could explain the rapid 1-D growth observed in micrometer-sized filamentary crystals, or "whiskers", of metals and semiconductors under low supersaturation.[14−16] According to Frank's mechanism of spiral crystal growth,[17,18] when a screw dislocation meets a crystal surface, it creates a permanently exposed spiral step[19] that accommodates adsorbed atoms and becomes a self-perpetuating spiral growth front. In the original works elucidating the VLS growth mechanism by Wagner and Ellis, extensive effort was made to rule out dislocation as the driving force in metal-catalyzed silicon whiskers,[20] which has since become the classic example of VLS growth. Despite Sears' satisfactory explanation

(1) Xia, Y.; Yang, P.; Sun, Y.; Wu, Y.; Mayers, B.; Gates, B.; Yin, Y.; Kim, F.; Yan, H. *Adv. Mater.* **2003**, *15*, 353–389.
(2) Lieber, C. M. *MRS Bull.* **2003**, *28*, 486–491.
(3) Law, M.; Goldberger, J.; Yang, P. D. *Annu. Rev. Mater. Res.* **2004**, *34*, 83–122.
(4) Yang, P. *MRS Bull.* **2005**, *30*, 85–91.
(5) Wang, Z. L. *Annu. Rev. Phys. Chem.* **2004**, *55*, 159–196.
(6) Li, Y.; Qian, F.; Xiang, J.; Lieber, C. M. *Mater. Today* **2006**, *9*, 18–27.
(7) Lieber, C. M.; Wang, Z. L. *MRS Bull.* **2007**, *32*, 99–108.
(8) Schmitt, A. L.; Higgins, J. M.; Szczech, J. R.; Jin, S., *J. Mater. Chem.* **2009**, DOI: 10.1039/b910968d.
(9) Wagner, R. S.; Ellis, W. C. *Appl. Phys. Lett.* **1964**, *4*, 89–90.
(10) Morales, A. M.; Lieber, C. M. *Science* **1998**, *279*, 208–211.
(11) Trentler, T. J.; Hickman, K. M.; Goel, S. C.; Viano, A. M.; Gibbons, P. C.; Buhro, W. E. *Science* **1995**, *270*, 1791–1794.
(12) Wang, F. D.; Dong, A. G.; Sun, J. W.; Tang, R.; Yu, H.; Buhro, W. E. *Inorg. Chem.* **2006**, *45*, 7511–7521.
(13) Persson, A. I.; Larsson, M. W.; Stenstrom, S.; Ohlsson, B. J.; Samuelson, L.; Wallenberg, L. R. *Nat. Mater.* **2004**, *3*, 677–681.
(14) Sears, G. W. *Acta Metall.* **1953**, *1*, 457–459.
(15) Sears, G. W. *Acta Metall.* **1955**, *3*, 361–366.
(16) Sears, G. W. *Acta Metall.* **1955**, *3*, 367–369.
(17) Burton, W. K.; Cabrera, N.; Frank, F. C. *Philos. Trans. R. Soc., A* **1951**, *243*, 299–358.
(18) Markov, I. V. *Crystal Growth For Beginners: Fundamentals of Nucleation, Crystal Growth, and Epitaxy*, 1st ed.; World Scientific Publishing Co.: Singapore, 1995.
(19) Frank, F. C. *Adv. Phys.* **1952**, *1*, 91–109.
(20) Wagner, R. S.; Ellis, W. C.; Jackson, K. A.; Arnold, S. M. *J. Appl. Phys.* **1964**, *35*, 2993–2301.

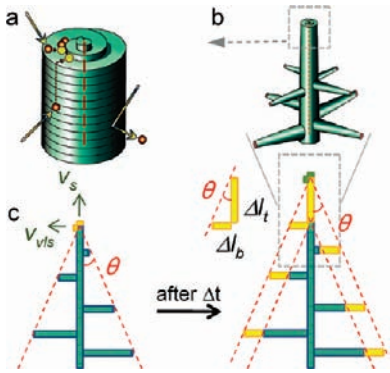

Figure 1. Schematic illustration of the growth process of a PbS nanowire pine tree nanostructure. (a) Anisotropic nanowire growth driven by screw dislocation growth spiral at the magnified trunk tip. (b) Three-dimensional representation of the tip region of a tree highlighting that the fast-growing trunk is driven by a screw dislocation while the branches are driven by VLS mechanism. (c) The tree evolves progressively leading to the formation of a cone angle (θ) of the outer envelope that represents the relative growth rate (trunk versus branch, or $v_s/v_{vls} = \cot\theta$). Panels a and b are reproduced from ref 21; copyright by AAAS.

for whisker growth kinetics, the dislocation driven mechanism has not been widely accepted or discussed in modern nanowire literature.[1]

We have recently reported lead sulfide (PbS) nanowires with morphologies resembling "pine trees" synthesized via chemical vapor deposition (CVD) and reestablished the screw dislocation nanowire growth mechanism.[21] Similar morphology was also reported by Cui and co-workers for lead selenide (PbSe) nanowires.[22] In contrast to previous PbS or PbSe nanowire growth via CVD reactions with or without intentional metal catalysts,[23−26] this tree morphology is formed by a combination of screw dislocation-driven nanowire growth that produced long and twisted "trunk" nanowires and a simultaneous self-catalytic VLS mechanism that resulted in epitaxial "branch" nanowires,[21,22] as illustrated in Figure 1. The expected spiral growth front at the tip of the trunk nanowire due to screw dislocation results in 1-D growth (Figure 1a). Lead particles generated in situ are suggested to be a self-catalyst to enable VLS growth of the branches (Figure 1b) that grow epitaxially off the trunk.[21,24] The large difference in nanowire growth rates of these mechanisms (v_{vls} for VLS, v_s for dislocation-driven) is easily visualized by the evolution of the highly anisotropic shape of the trees (Figure 1c). Specifically, the ratio of the growth rates (trunk versus branch, or v_s/v_{vls}) is equal to the cotangent of the cone angle ($\cot\theta$) of the outer envelope of the trees. The rotating sets of epitaxial branch nanowires clearly illustrate the twisting behavior of the trunk, which is due to a torque produced by the stress field of an axial dislocation with a screw component in the nanowire, a phenomenon known as the Eshelby twist.[27] The existence of a dislocation in the trunk has been proven using diffraction contrast transmission electron microscopy (TEM); the branches are free of screw dislocations as revealed with the same technique.[21,28]

The screw dislocation-driven nanowire growth mechanism deserves further investigation, because it can also be applicable in a variety of materials and may have been far underappreciated as a viable path of creating 1-D nanostructures without catalysts. The ability to control the formation of hierarchical nanostructures with increasing structural complexity, as seen in these pine tree nanowires, can potentially empower increasing functionalities and enhance applications such as solar energy conversion[29,30] and 3-D nanoelectronics. Furthermore, because dislocations are known to significantly influence many aspects of physical properties of materials, such as electronic, magnetic, and thermal properties,[31−34] the dislocations in these nanowires may possess interesting physical properties, which if understood and well-controlled could lead to novel device applications. Nanostructures of PbS pine trees represent a convenient and suitable platform for investigating dislocation-driven nanowire growth, because the highly anisotropic tree shape and rotating branches with Eshelby twist provides direct visual evidence of dislocations with screw component. This is important because dislocations are not trivial to observe routinely with large numbers of samples using conventional characterization techniques, such as high-resolution and diffraction contrast TEM.[28] The large yield of pine tree nanostructures also facilitates large scale investigation of the characteristics of the dislocation-driven nanowire growth.

This article reports the findings from a comprehensive study of the evolution of the pine tree nanowire nanostructures under the influence of hydrogen, temperature, pressure, and silicon in the reaction system. We have investigated how these experimental parameters can be tuned to control dislocation-driven and VLS nanowire growth mechanisms, leading to complex PbS nanostructures of predictable morphologies. The basic characteristics of dislocation-driven nanowire growth are summarized. In the Discussion section, we elucidate the chemical insights gleaned from this specific PbS nanowire growth system that has yielded surprisingly rich and intriguing morphologies. We further connect the observations to classical crystal growth theory,[17,18] which states that supersaturation plays the central role in differentiating the three distinctive growth regimes of dislocation-driven, layer-by-layer, and dendritic growth, and dislocation-driven is most favored at low supersaturation. We try to present a general framework of understanding on the screw-dislocation driven nanowire growth mechanism in the context of fundamental crystal growth theory.

2. Results

Through numerous reactions (exceeding 400), we have established a set of typical reaction conditions for synthesizing

(21) Bierman, M. J.; Lau, Y. K. A.; Kvit, A. V.; Schmitt, A. L.; Jin, S. *Science* **2008**, *320*, 1060–1063.
(22) Zhu, J.; Peng, H. L.; Marshall, A. F.; Barnett, D. M.; Nix, W. D.; Cui, Y. *Nat. Nanotechnol.* **2008**, *3*, 477–481.
(23) Ge, J.-P.; Wang, J.; Zhang, H.-X.; Wang, X.; Peng, Q.; Li, Y.-D. *Chem.—Eur. J.* **2005**, *11*, 1889–1894.
(24) Bierman, M. J.; Lau, Y. K. A.; Jin, S. *Nano Lett.* **2007**, *7*, 2907–2912.
(25) Fardy, M.; Hochbaum, A. L.; Goldberger, J.; Zhang, M. M.; Yang, P. *Adv. Mater.* **2007**, *19*, 3047–3051.
(26) Zhu, J.; Peng, H.; Chan, C. K.; Jarausch, K.; Zhang, X. F.; Cui, Y. *Nano Lett.* **2007**, *7*, 1095–1099.
(27) Eshelby, J. D. *J. Appl. Phys.* **1953**, *24*, 176–179.
(28) Williams, D. B.; Carter, C. B. *Transmission Electron Microscopy: A Textbook for Materials Science*, 1st ed.; Plenum Press: New York, 1996.
(29) Bierman, M. J.; Jin, S. *Energy Environ. Sci.* **2009**, *2*, 1050–1059.
(30) Lau, Y. K. A.; Chernak, D. J.; Bierman, M. J.; Jin, S. *J. Mater. Chem.* **2009**, *19*, 934–940.
(31) Matare, H. F. *Defect Electronics in Semiconductors*; Wiley-Interscience: New York, 1971.
(32) Hogarth, C. A.; Baynham, A. C. *Proc. Phys. Soc.* **1958**, *71*, 647–653.
(33) Yu, K. K.; Jordan, A. O.; Longini, R. L. *J. Appl. Phys.* **1967**, *38*, 572–582.
(34) Szot, K.; Speier, W.; Bihlmayer, G.; Waser, R. *Nat. Mater.* **2006**, *5*, 312–320.

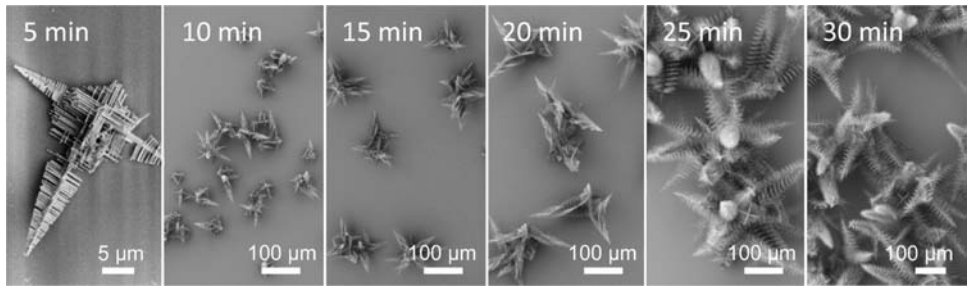

Figure 2. SEM images showing the progression of PbS nanowire pine trees over reaction time.

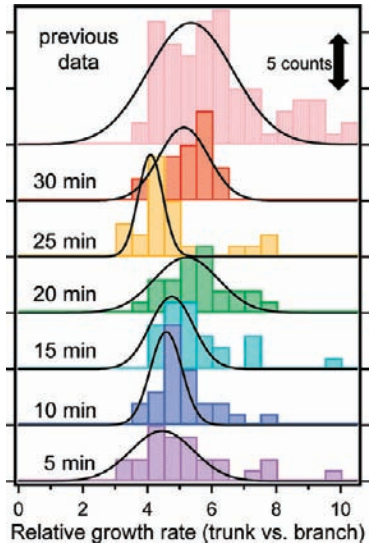

Figure 3. Histograms comparing the distributions of relative growth rate (trunk versus branch) by measuring the cone angles for 25 trees grown for each of the six time durations, showing that the trunk (dislocation-driven) consistently grows at about 5 times faster than the branch.

PbS nanowire pine trees via CVD of $PbCl_2$ and S precursors under hydrogen co-flow, as described in the Experimental Section. If not stated otherwise, this was the "typical reaction condition" used in our study. The geometrical analysis of trees was carefully conducted under guidelines that are explained in the Instrumentation and Methods subsection.

2.1. Cone Angle Analysis. To more fully investigate the evolution of the trees, typical reactions were terminated at 6 different times from 5 to 30 min, and the samples were examined using scanning electron microscopy (SEM) (Figure 2) and optical microscopy to measure and compare the cone angles (θ) and lengths of a large number of trees. The cone angle is converted into relative growth rate (trunk versus branch, $v_s/v_{vls} = \cot\theta$) as discussed above.[21] From cone angle measurements of 150 trees (Figure 3), it is clear that the distributions of relative growth rates are similar and centered around 5 throughout the course of the reactions and also agree with measurements published previously.[21] This means that, throughout the entire reaction, the trunks grow at about 5 times of the rate of the branches, and the tree shape persists.

2.2. Growth Rate Analysis. Measurements on 315 trees, as tabulated in Table 1, indicate that the length of the trees increases linearly with respect to time (Figure 4), suggesting a constant growth rate of the trunk of about 6 μm/min (6.4 $\pm$ 0.2 μm/min by fitting the arithmetic averages of tree lengths and 6.2 $\pm$ 0.3 μm/min by fitting the Gaussian averages of the tree lengths) under the typical reaction conditions at 600 °C and 900 Torr. This trunk growth rate, in combination with the cone angle measurement, yields a VLS-driven branch nanowire growth rate of about 1.2 μm/min. Since linear extrapolation shows only a small offset from the origin (Figure 4b), it seems that the trees

Table 1. Arithmetic Averages and Gaussian Means of Tree Length and Relative Growth Rate (Trunk versus Branch) as a Function of Growth Time

	length of tree (μm)		relative growth rate (trunk vs branch)	
growth time (min)	average (SD)	Gaussian mean (SD)	average (SD)	Gaussian mean (SD)
5	30 (15)	23 (16)	5.3 (1.5)	4.5 (1.4)
10	54 (14)	46 (11)	5.1 (1.0)	4.6 (0.7)
15	90 (21)	88 (23)	5.5 (1.3)	4.8 (0.9)
20	118 (30)	105 (23)	5.6 (1.0)	5.2 (1.4)
25	155 (43)	150 (41)	4.8 (1.3)	4.1 (0.5)
30	188 (57)	175 (34)	5.1 (0.7)	5.1 (1.1)

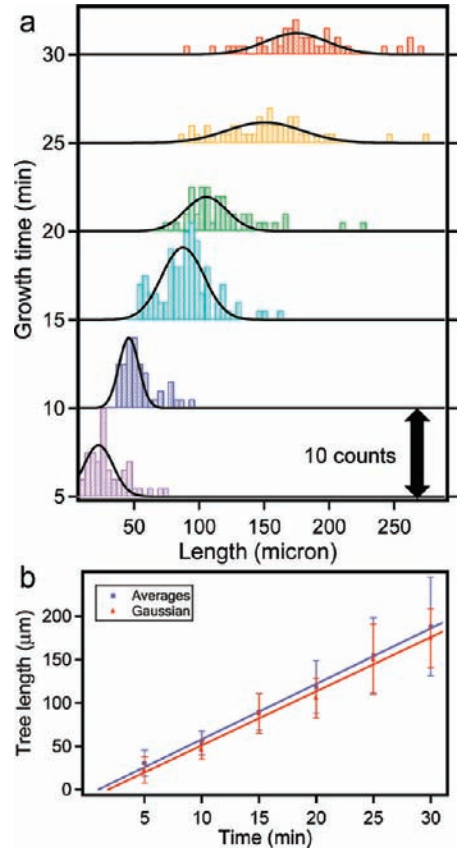

Figure 4. (a) Stacked histograms showing the evolution in the tree length distributions over time. (b) Least-square fits of tree length as a function of reaction time. The square/blue data points represent the arithmetic averages of trees grown for the specified time period. The triangular/red data points represent the Gaussian means from the same data set. Error bars are standard deviations.

start growing near the beginning of the reactions as defined by the onset of the hydrogen flow. In the initial works by Sears, it was hypothesized that the growth rate of screw dislocation-driven whiskers should be exponential initially until reaching a certain high rate that is equal to the diffusion rate of the precursor species on the crystal faces.[15] This was later confirmed in mercury whiskers using field emission observations.[35] Such behavior was not clearly observed in the growth rate of PbS trees, likely because the time resolution here is not sufficient to differentiate the initial period when the nanowire growth rate was increasing exponentially. However, the small positive time intercepts by the fitted linear rate curve is not in conflict with the hypothesis of initial exponential growth (the alternative explanation is a short induction period before the growth). The increasing length distributions with longer reaction times are expected because small differences in growth rates between different trunks would lead to a wider distribution as time progresses. However, by and large all distributions are Gaussian and do not spread out over the entire range. This suggests that all PbS trees are initiated at once, which appears to be correlated with the onset of the hydrogen flow at time zero (see more below).

2.3. Effects of Hydrogen on the Formation of Pine Tree Nanowires. From our earlier studies of hyperbranched PbS and PbSe nanowires, it is known that product morphology in this chemical system is highly sensitive to hydrogen flow.[21,24] If no hydrogen is used, only sparse small crystals can be reliably obtained. At 600 °C and 900 Torr, flowing hydrogen at 1.0 sccm for only the first minute of the reaction yields hyperbranched nanowires (Figure 5a). Almost exclusively pine tree nanowire morphologies can be produced when 1.0−2.5 sccm of hydrogen is flowed throughout the reaction (Figure 5b). Further increasing the hydrogen flow to 9−20 sccm yields mixtures of a variety of morphologies that include trees, hyperbranched nanowires, and small cubes (Figure 5c).

More intriguing and informative were the experiments where the hydrogen flow was turned "on" (at 1.5 sccm) and "off" (at 0 sccm) at different times in increments of 5 min while the rest of the conditions were kept standard, as schematically illustrated in Figure 6a for 10 selected hydrogen flow profiles (**a1**−**a10**). The measured total tree length distributions corresponding to these profiles are displayed in Figure 6b in three groups, **a1**−**a4**, **a5**−**a7**, and **a8**−**a10**, organized by the *total* effective hydrogen flow time of 10, 15, and 20 min, respectively. By comparing these distributions of tree lengths to the results from reactions with continuous hydrogen co-flow terminated at different times (Figure 4 and Table 1), a few observations can be made. First, the trees seem to only significantly elongate in the period when hydrogen flow is present. For example, in reaction **a1**, even though the entire reaction lasts for 15 min, hydrogen is only co-flowed in the last 10 min. The resulting trees (Figure 6c) have an average length of about 48 μm (Figure 6b, **a1**), which is similar to trees grown for a total of 10 min continuously under typical conditions. A similar trend is observed in 30-min reactions in which hydrogen is removed in the final 10 min period, as exemplified by reaction **a8** (Figure 6d). In other words, regardless of the total reactions times and when the hydrogen-off periods occur, the same *total* duration of hydrogen flow always yields trees with the same total average length within statistical errors. Interestingly, when hydrogen flow is turned off in the middle of the reaction, two distinct distributions

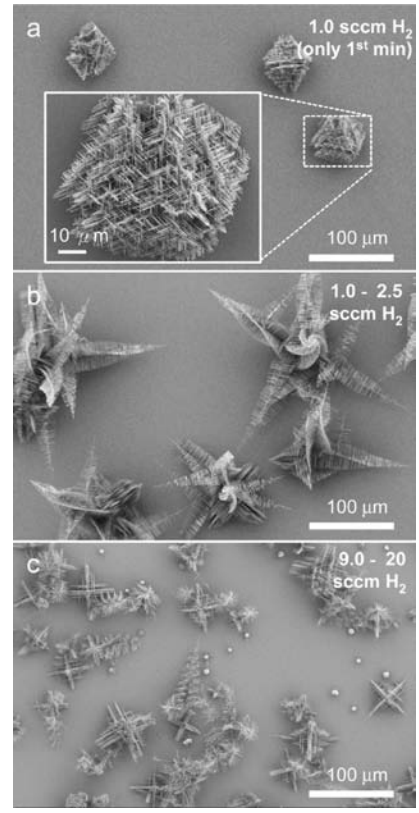

Figure 5. Global effects of hydrogen flow on the morphology of PbS nanowires or other CVD products. (a) Clusters of hyperbranched nanowires formed with 1-min initial hydrogen flow at 1.0 sccm. (b) Exclusively tree morphology resulting from 1.0−2.5 sccm constant flow of hydrogen. (c) Mixtures of trees, hyperbranched clusters, and small cubes from 9.0−20 sccm of hydrogen flow.

of tree lengths are sometimes observed. For a sample produced when 10 min of hydrogen is followed by 5 min with no hydrogen and then an additional 5 min with hydrogen again (profile **a7**), trees about 90 μm long can be observed (Figure 6e). These trees are likely to have nucleated at the very beginning and grow in both periods of hydrogen flow. Additionally, many smaller trees with length of ~30 μm can also be found, often growing out of hyperbranched clusters (Figure 6f). This suggests that the second onset of hydrogen flow initiates more trees. Following this hypothesis, bimodal distributions of tree lengths should be expected for any reaction with a period of no-hydrogen flow in the middle (**a2**, **a5**−**a7**, **a9**, **a10**). This appears to be the case for profiles **a6**, **a7**, and **a10** but not **a2**, **a5**, and **a9**. The two groups of trees are not always easily differentiated by statistics because of the overlapping intrinsic distributions of tree lengths, and/or the shorter trees might also be overwhelmed and covered by longer ones so that representative surveys cannot be conducted.

The formation of pine trees essentially requires the introduction of dislocations with screw components and a reaction environment that encourages the growth of both dislocated trunks and VLS branches. The observations above collectively imply that the introduction of dislocations is likely empirically triggered by the onset of hydrogen flow in this CVD reaction system, and maintaining hydrogen flow at an appropriate level (1.0−2.5 sccm) is essential to provide an environment that promotes dislocation-driven tree growth. When hydrogen is not supplied in the middle of a reaction, the suppressed hydrogen level may lead to the temporary halt of tree growth and the

(35) Gomer, R. *J. Chem. Phys.* **1958**, *28*, 457–464.

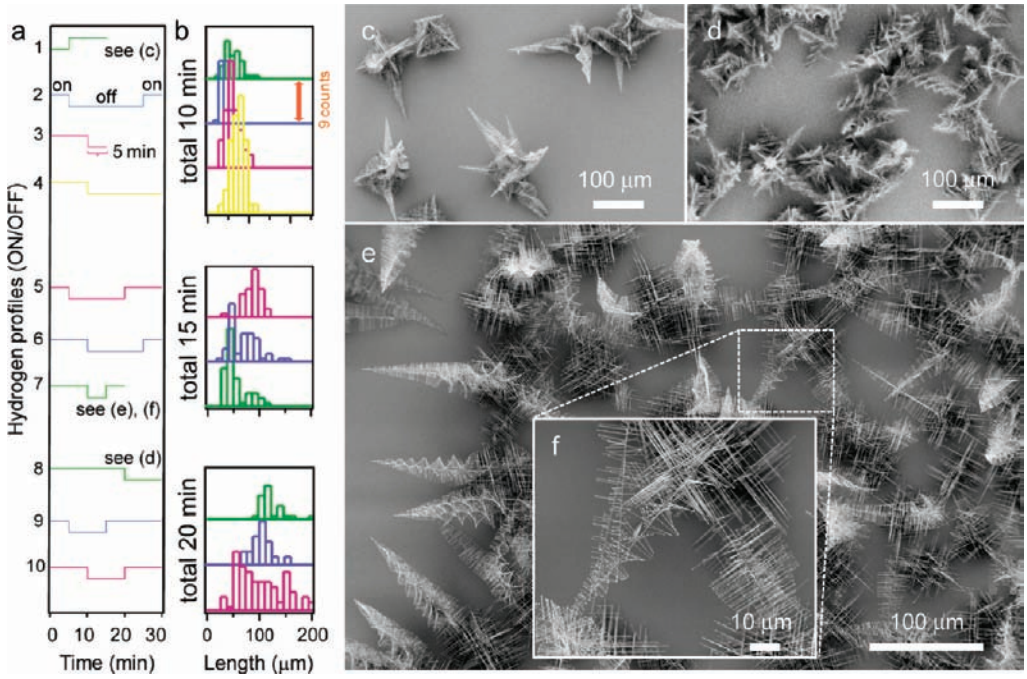

Figure 6. Effects of hydrogen flow modulation on the distribution of tree lengths and morphology. (a) Hydrogen flow profiles (**a1**−**a10**) with (b) histograms showing the corresponding distribution of trees (25−90 trees measured for each profile) are organized according to the total effective flow time of hydrogen (10, 15, and 20 min from top to bottom). Representative SEM images of trees from reaction **a1**, **a8**, and **a7** are displayed in panels c, d, and e/f, respectively.

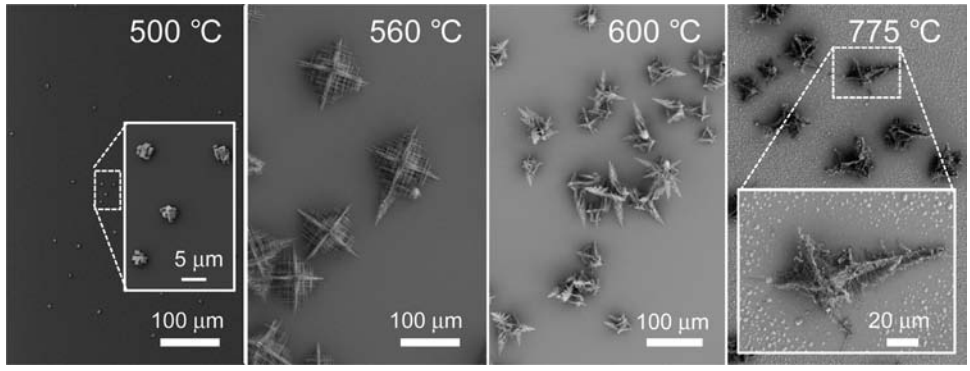

Figure 7. SEM images of typical deposition morphology at different temperatures.

formation of some hyperbranched nanowires as seen in Figure 6e/f. However, it seems that dislocation growth can resume once a favorable hydrogen flow condition returns. The return of hydrogen also presents another opportunity for introduction of dislocations which could lead to initiation of more trees.

2.4. Effects of Temperature. Figure 7 summarizes the influence of growth temperature on tree morphology. When temperature is too low (500 °C), no nanowires are formed at all, only particles. At about 560 °C, hyperbranched nanowires and some trees can be produced. The formation of pine tree morphology is highly favorable only at about 600−650 °C. Excessively high temperature (775 °C) yields lots of particles and messy tortuous trees that are probably heavily etched and damaged. The growth rate of the tree (trunk) is observed to increase with respect to temperature when the rest of the conditions are kept constant and standard (Figure 8). Within the temperature range of 570−609 °C, the growth rate increases at about 0.16 μm/min/°C.

2.5. Effects of Pressure. Pressure change and modulation primarily have a pronounced impact on the branching behavior

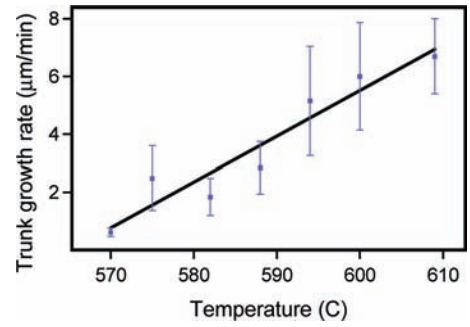

Figure 8. Trunk nanowire growth rate as a function of temperature from 570 to 609 °C.

of trees. Figure 9a displays the morphology obtained when pressure is dropped from 900 to 600−650 Torr during the middle of a reaction for 5 min and then brought back to 900 Torr for another 5 min. Many trees have "2-stage" branching (Figure 9b), where branches become progressively shorter from

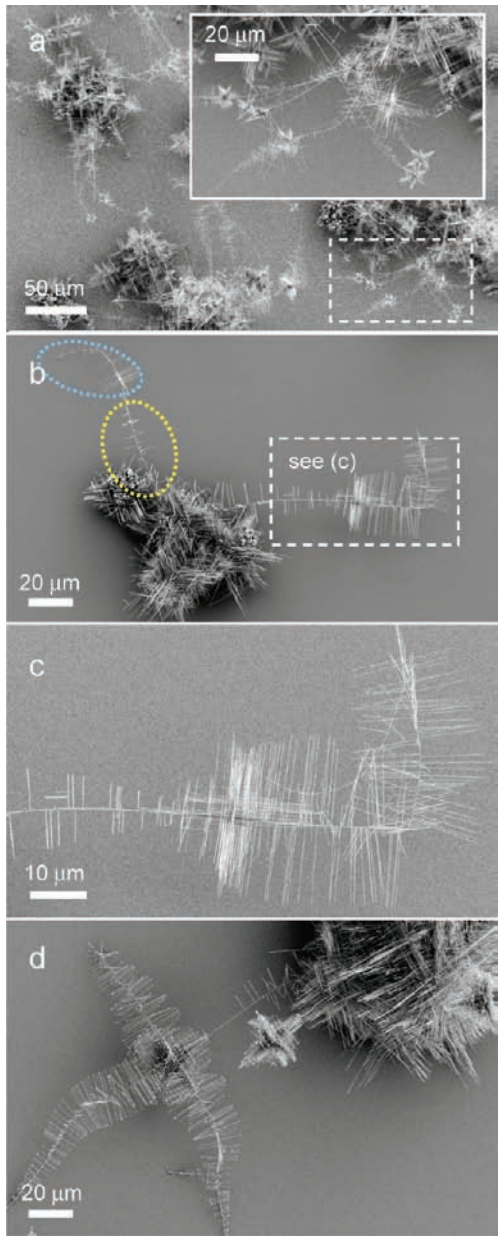

Figure 9. SEM images showing the modulated branching in the trees due to pressure changes. (a) Extensive 2-stage branching behavior, which becomes clearer in magnified view (inset). (b) First stage of branching (lower yellow oval) is terminated during pressure drop, but the dislocation-driven trunk can still grow and new branching (upper blue oval) can occur when pressure is brought back to normal level (900 Torr). Selected area in (b) is magnified in (c) to show that sometimes the recurrence of branching is accompanied by a burst of orthogonal branching. (d) A rare example in which the new trees seem to have nucleated and grow when pressure is returned to normal.

the bottom up along the trunk and then new branching recurred (circled in blue), but the previously growing branches (circled in yellow) apparently have stopped growing. The reduction in pressure probably results in evaporation of lead catalyst at the branch tips, which permanently terminates the branch growth, while trunk nanowires still have "living" growth fronts provided by dislocation spirals. When the pressure is brought back to "standard" level (900 Torr), the tree growth resumes with new branches nucleating and growing on only the newer segment of the trunks. Dense orthogonal clusters resembling hyperbranched nanowires sometimes grow off from the trunk at the

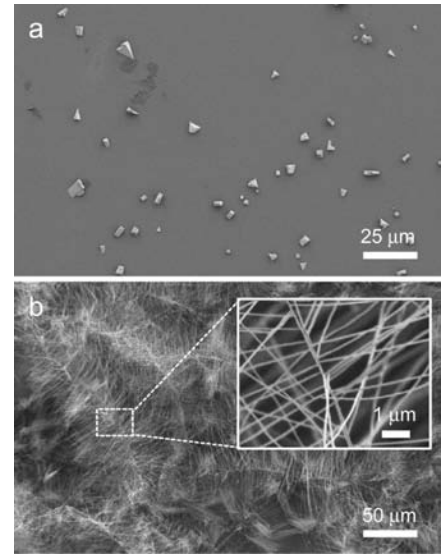

Figure 10. Role of silicon in the CVD growth of PbS nanowires. (a) On glass substrates without any form of freshly exposed silicon in proximity, only small PbS crystals can be deposited. (b) Nanowire trees (magnified to highlight rotating branches in inset) can be easily obtained on glass substrates in the presence of fresh silicon.

second initiation of branching (Figure 9c). Occasionally, the return of higher pressure seems to initiate additional pine trees (Figure 9d).

2.6. Role of Silicon and Growth on Various Substrates. As mentioned in our previous reports, we have consistently observed that freshly exposed silicon from the edges of silicon substrates covered with silicon oxide is essential in reproducibly generating trees and PbS nanowires of other morphologies.[21,24] The reproducibility of nanowire growth seems to be sensitive to the quantity of fresh silicon available. Simultaneous use of multiple small silicon substrates or the use of a silicon substrate with multiple scratches on the surface (to expose more fresh silicon) can also produce comparable amount of trees. In the absence of any form of elemental silicon, such as when only glass slides were used as the substrates, only micrometer-sized PbS crystals are obtained in otherwise identical synthesis conditions (Figure 10a). However, extensive growth of trees (though with less order) can also be produced on small glass substrates (microscope slides) if they are in close proximity to a thin slice of silicon substrate that has a high edge-to-interior ratio or even silicon powder (Figure 10b). On the other hand, some oxide surface is still needed, since when silicon substrates covered with native oxides or no oxide (freshly etched) are used, only bulk particles or thin films are deposited. Silicon oxide provides an inert surface for PbS deposition. The role of silicon seems to be the creation of silicon disulfide (SiS_2). The importance of this step in the growth of PbS naowires will be further examined in the Discussion section.

In general, PbS nanowires can be formed with high yields on other substrates, such as NaCl, mica, and TiO_2, if they are placed onto or side-by-side with a silicon substrate, similar to the case for glass slides.[30] Attempts to grow epitaxially aligned PbS trees by introducing crystalline substrates that are expected to have lattice match with PbS have been unsuccessful so far regardless of the hydrogen flow profiles employed,[30] perhaps because the conditions that promotes epitaxial growth produces registry between nucleated particles and does not favor the introduction of dislocations. In contrast, hyperbranched PbS

nanowires without dislocations can be readily grown epitaxially on single crystalline NaCl, TiO_2 rutile (001), and muscovite mica.[30]

3. Discussion

In the early studies of whisker growth by Sears and others, it was observed that supersaturation has a huge influence on growth morphology.[17,18,36,37] In classical crystal growth theory, supersaturation is defined as the ratio between actual vapor pressure (concentration) and the equilibrium vapor pressure (concentration) of the species being crystallized from the vapor (solution) phase, or more rigorously, the natural logarithm of this ratio (which is approximately the same at low value). It basically describes the thermodynamic driving force for formation of a solid from its vapor (or solution). According to the classical crystal growth theory,[17,18] the three distinctive crystal growth regimes, dislocation-driven, layer-by-layer, and dendritic, require progressively higher critical supersaturations and have progressively larger growth rates in the regimes where each of them dominates. In the low supersaturation regime, dislocation-driven growth dominates, i.e., its growth rate is much faster than the other modes. VLS growth is in fact a special layer-by-layer growth mode mediated by catalyst where crystal precipitates from the solution of the catalytic liquid droplet instead of from vapor to solid directly. The concept of supersaturation has been applied to the discussion of whisker growth from purely physical condensations, such as the condensation of Hg vapor to form Hg whiskers, in the original work by Sears.[15] Understanding supersaturation for the case at hand is much more complex because the PbS compound is formed via chemical reaction(s), and there are multiple chemical species and chemical reactions involving H_2 and temporal changes during the course of reactions under gas flow, yet this case can still be viewed in a similar framework. The concentrations of the precursors ($PbCl_2$ and S or H_2S) can be taken as the proxy for the supersaturation or the thermodynamic driving force of the chemical reaction(s) that form PbS should now be considered.

3.1. Chemical Reactions and Species Involved. To explain the effects of hydrogen and thus supersaturation on the growth of PbS nanowires, we need to first consider the chemical reactions and species in the reactor. It has been observed that little deposition of small crystals resulted without the presence of hydrogen flow. In this case, the reaction that could lead to the formation of PbS is

$$PbCl_2(s) + 1/2S_2(g) = PbS(s) + Cl_2(g) \quad (1)$$

This reaction, however, is thermodynamically unfavorable with a calculated free energy of reaction ΔG at 900 K of 143.77 kJ/mol using tabulated values of standard free energy of formation[38] (see Table S1 in Supporting Information for list of values). The temperature in the reaction zone at the center of the furnace ranges from 873 K (600 °C) to 923 K (650 °C) for the typical PbS tree syntheses. Estimated free energy values at 873 K (600 °C), also listed in Table S1, clearly show that using thermodynamic values at 900 K does not cause a significant difference for the purpose of this discussion.

The addition of hydrogen, in the presence of sulfur, leads to the highly favorable formation of hydrogen sulfide (H_2S) upstream of the reaction zone ($\Delta G = -39.045$ kJ/mol at the mouth of the furnace with about 187 °C):

$$H_2(g) + S(s) = H_2S(g) \quad (2)$$

The availability of H_2S is expected to make the formation of PbS more favorable via this reaction:

$$PbCl_2(s) + H_2S(g) = PbS(s) + 2HCl(g) \quad (3)$$

which is predicted to occur spontaneously, with a ΔG of -10.65 kJ/mol at 900 K. This small value of free energy of formation is interesting because a chemical reaction that is close to equilibrium is equivalent to a low supersaturation in simple physical condensation. Despite the lack of instrumentation capability to confirm the presence of H_2S directly, the smell of "rotten eggs" that is characteristic of H_2S was occasionally noticed when the CVD reactor was vented and opened to air at the end of reactions. If we assume equilibrium reaction between sulfur and hydrogen with a partial pressure of 8.9 Torr (for 1.5 sccm flow rate out of 150 sccm argon flow rate at a total pressure of 900 Torr) at the temperature at the position of the sulfur boat (about 187 °C), estimation of the vapor pressure of H_2S yields an unrealistically large value. Even if we assume hydrogen is used up (limiting) in a quantitative reaction 2, we can still expect a high partial pressure of H_2S at 8.9 Torr (1.18×10^3 Pa). The calculations herein are often limiting estimates because of the flowing environment and varying temperatures.

However, the critical requirement of fresh silicon, as discussed in section 2.6, prompts us to consider the reaction between silicon and H_2S to form silicon sulfide (SiS_2):

$$2H_2S(g) + Si(s) = SiS_2(s) + 2H_2(g) \quad (4)$$

This reaction, with a calculated ΔG of -109.06 kJ/mol at 900 K, is thermodynamically much more favorable than the formation of PbS via reaction 3 in the reaction zone. When the as-generated H_2S is transported to the reaction zone, some of it will contribute to the formation of PbS, but a large portion is expected to be consumed by reacting with the exposed silicon from substrate edges. It was observed that after successful PbS nanowire growth reactions the exposed silicon surface was always covered by gray deposits, which were suspected to contain SiS_2. Powder X-ray diffraction (PXRD) of this deposit (Figure S1, Supporting Information) showed a small fraction of the diffraction peaks matching those of SiS_2 phase together with PbS phases in larger quantity (present as films or cubes). The apparent weak diffraction peaks from SiS_2 is perhaps not surprising given that the commercial SiS_2 powder also appears to be poorly crystalline. It is also possible that SiS_2 quickly hydrolyzes in moist air due to this highly thermodynamically favorable reaction with a calculated ΔG of -242.56 kJ/mol at 900 K (or -253.33 kJ/mol at 300 K):

$$SiS_2(s) + 2H_2O(g) = SiO_2(s) + 2H_2S(g) \quad (5)$$

More importantly, reactions where only SiS_2 was placed next to a glass slide substrate with the presence of hydrogen flow have produced PbS nanowire trees as well. In this case, the SiS_2 reacts with H_2 to produce the low concentration H_2S "buffer" (via reverse reaction 4) necessary for the formation of PbS

(36) Gibbs, J. W.; Bumstead, H. A.; Longley, W. R.; Van Name, R. G. *On the Equilibrium of Heterogeneous Substances, Collected Works*; Longmans, Green and Co.: New York, 1928.
(37) Bolling, G. F.; Tiller, W. A. *Metallurgical Society Conferences [Proceedings]* **1961**, *12*, 97–119.
(38) Chase, M. W. J. *NIST-JANAF Thermochemical Tables*, 4th ed.; American Institute of Physics: Woodbury, NY, 1998.

(reaction 3). More intriguingly, if SiS_2 was placed onto a glass slide substrate, plenty of PbS nanowires together with some cubes can still be produced without hydrogen flow, so long as some minute amount of water is present in the reactor. This moisture could come from heating up about 80 mg of the hydrated form of the desiccant "Drierite" (mainly $CaSO_4 \cdot 2H_2O$ that is in pink color due to 2% $CoCl_2$ indicator) outside the mouth of the tube furnace (at about 70 °C). In this case, H_2S is generated via reaction 5. In fact, sometimes SiS_2 on glass substrates alone without the intentional introduction of water can result in sparse nanowire growth. This is likely due to the moisture in the air or absorbed on instruments and reagents. This might also explain the success of the earlier report of PbS nanowire growth[23] and our occasional success of synthesizing PbS nanowires without intentionally introducing hydrogen flow. In all of the CVD reactions using $PbCl_2$ and S precursors, SiS_2 can always be formed via the reaction of Si with evaporated (or sublimed) S_2 vapor directly since this SiS_2 formation reaction is rather favorable. When a few drops of water were added into a boat upstream of the CVD reactions together with SiS_2 on glass substrates, prodigious amounts of PbS cubes were formed, consistent with the observation for reactions with large amount of hydrogen flow (beyond 20 sccm and Figure 5c). Essentially, SiS_2 is a viable precursor to PbS nanowire growth through either reaction 5 or reverse reaction 4. All of these observations confirm that SiS_2 is involved during PbS nanowire growth.

3.2. True Supersaturation and Estimate of the Kinetics of PbS Nanowire Growth. In this chemical system, the partial pressure of hydrogen is expected to be a key in governing the thermodynamic driving force for production of H_2S and therefore generation of PbS. In other words, it may be regarded as a main determining factor of supersaturation. However, the sensitive substrate dependence demonstrates that merely controlling hydrogen flow rate is not the whole story. The reaction of forming SiS_2 (reaction 4) is thought to consume a significant portion of H_2S and be crucial for setting the H_2 concentration. In fact, a more conceptually useful description of the chemical reactions might be that the "main" reaction is the formation of SiS_2 (reaction 4) and the formation of PbS (reaction 3) is a "side" reaction with its reactant H_2S "buffered" at low concentration by reaction 4. Now when the reaction 4 involving H_2S is considered and a steady state partial pressure of 8.9 Torr is assumed for hydrogen (a hydrogen flow rate of 1.5 sccm out of a total flow rate of 151.5 sccm at a total pressure of 900 Torr, which is obviously an overestimate since this assumes no hydrogen consumption), the upper limit of the H_2S partial pressure is much reduced to about 0.8 Pa using the equilibrium constant of 2.13×10^6 for reaction 4 at 900 K. From the kinetic theory of gases, H_2S is expected to have a molecular flux ($J = pN_A/(2\pi M_w RT)^{1/2}$) of about 1.2×10^{22} molecules/m$^2 \cdot$s at such pressure. That means a typical PbS nanowire with a 100 nm diameter would be struck by 9.6×10^7 H_2S molecules per second at its tip. It is interesting to see that on almost the same order of magnitude, about 1.5×10^8 molecular units of PbS per second are required to account for the observed dislocation-driven trunk nanowire growth rate of 6 μm/min (section 2.2). On the other hand, the vapor pressure of $PbCl_2$ at 600 °C and 900 Torr total pressure is about 1.2 Torr, which means about 6.8×10^9 $PbCl_2$ molecules strike a nanowire tip per second and is much more than what is necessary to account for the nanowire growth rate. In comparison with Sears' kinetic treatment in the simple one-component physical condensation for the growth of Hg whiskers,[15] the reactions here are much more complex, and therefore the estimate is very crude. However, at least there is some qualitative agreement when (and only when) we assume H_2S pressure is suppressed by the SiS_2 formation reaction. More quantitative discussion requires much more controlled reactions with accurate measurements of species and possibly more refined theory as well.

If we assume that the self-perpetuating step of a screw dislocation is a "sink" of adatoms as pictured in Frank's spiral growth mechanism,[19] then the growth rate of a dislocated nanowire should be limited by the rate of supply of precursor molecules to the growth front.[15,17,35] From the kinetic analysis above, H_2S is the limiting reactant that controls the growth rate of dislocated PbS nanowires (the trunks in the PbS trees), while $PbCl_2$ is probably a reactant in excess and contributes to the extra Pb catalysts. For the VLS-driven branches, the observed growth rate is observed to be about 1 μm/min. Obviously, not all of the precursor molecules that strike the branch tips are immediately incorporated into PbS. This is perhaps not surprising as the VLS growth follows the layer-by-layer growth mechanism where the formation of two-dimensional nuclei can be a rate-determining step in crystal growth.

3.3. Initiation of Dislocation-Driven Nanowire Growth. Successful dislocation-driven nanowire growth needs at least the following three steps: (i) the emergence (or presence) of screw dislocations in the solid, (ii) evolution of the dislocation growth spirals on crystal facets into 1-D objects with the spiral on top, and (iii) suitable low supersaturation conditions that promote sustained dislocation-driven crystal growth so that it overtakes other growth modes. The observed nucleation of trees upon onset of hydrogen flow is possibly due to a sudden increase of supersaturation level that leads to rapid and "imperfect" depositions of PbS crystallites and films. The slightly mismatched crystalline grains at the boundary can lead to the creation of dislocations.[39] However, the sudden increase in H_2S is quickly subdued as silicon begins to react with H_2S, which reduces and then "buffers" the supersaturation at a lower level dictated by reaction 4. This reduced supersaturation is suitable for sustained dislocation-driven growth but not adequate for generating additional screw dislocations. This could explain why the constant flow of hydrogen (at optimal level, 1.0−2.5 sccm) does not continuously nucleate more trees over the course of a reaction, which would have led to much wider and non-Gaussian distributions of tree length in Figure 4. Why a second onset of hydrogen flow initiates more tree growth can be similarly explained.

The dislocation spirals on the face of crystals also need to evolve into 1-D cylinders. Two scenarios (Figure 11) are plausible: (i) In diffusion-limited spiral evolution (Figure 11, a−c),[40] the step growth (advance) rate increases with the increase of supersaturation (concentration), and very fast growth quickly depletes the precursors in nearby regions in a diffusion-limited environment, which then suppresses the step advance rate of those regions. A sudden increase in supersaturation helps to accentuate the contrast and differentiate the step growth at the very center of the growth spiral and step growth farther away so that the spiral "pulls into" a 1-D object. Once the geometrical difference is formed, a low and steady supersaturation is sufficient to maintain highly anisotropic growth so long as the supersaturation is below what is necessary for 2-D nucleation for layer-by-layer growth on the side wall of the cylinder

(39) Nabarro, F. R. N. *Theory of Crystal Dislocations*; Clarendon Press: Oxford, 1967.
(40) Brenner, S. S.; Sears, G. W. *Acta Metall.* **1956**, 268–270.

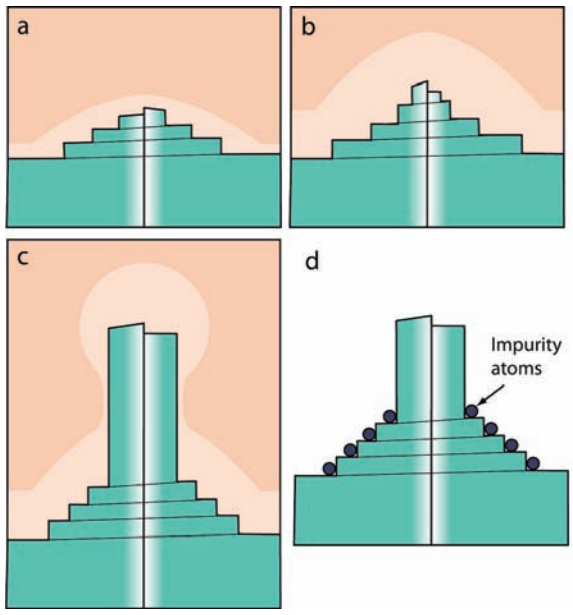

Figure 11. Schematic illustration of two possible situations where a dislocation growth spiral on a crystal face can evolve into a 1-D cylinder: (a−c) diffusion-limited, (d) impurity pinning.

(however, spiral growth at the base of the cylinder on the dislocation steps "left behind" can still proceed, but their growth rate is slower than that at the nanowire tip). The diameter of the nanowire formed this way is likely determined by the supersaturation (concentration) and/or the rate of sudden supersaturation increase. (ii) The second possibility is an "impurity pinning" mechanism first suggested by Amelincks.[41] In this case, a small amount of impurity atoms or molecules can absorb onto the base crystal steps and thus "poison" the crystal growth by inhibiting the step advance. The newly emerged spiral steps near the dislocation core are less likely to be blocked by impurities (that have limited quantity). Therefore these fast moving steps "pile up" (become bunched) and force the growth spiral to wrap back on top of itself, therefore forming a 1-D cylinder. This possibility is likely more common in solution phase growth with "additives" but also possible in vapor phase growth.

3.4. Relationship between Dislocation-Driven and VLS Nanowire Growth. The next requirement after dislocation-driven nanowire growth is initiated is maintaining a low supersaturation favorable for dislocation-driven growth so that it dominates over (or at least is not overwhelmed by) other growth modes, such as VLS. This is achieved herein by setting H_2S concentration (pressure), which is fortuitously helped by SiS_2 whose formation reduces and stabilizes the H_2S concentrations. However, as demonstrated with various experiments, so long as H_2S can be generated and maintained at appropriate concentration, nanowire growth can proceed regardless of whether it comes from reaction of H_2 with S, SiS_2 with H_2, or SiS_2 with H_2O. For the first case, a continuous flow of hydrogen is still required to maintain the evolution of trees, which includes the advancement of trunks and branches and frequent creation of new branches, because hydrogen is required to produce H_2S at the appropriate supersaturation that is a limiting reactant for the growth of dislocated trunk nanowires. Without hydrogen, the trunk cannot grow at an appreciable rate, which explains why the trunk can only grow for as long as the effective flow time of hydrogen as demonstrated in Figure 6. This also explains why hyperbranched nanowires are predominantly observed with only a short bolus of hydrogen at the beginning, as discussed in section 2.3 and shown in Figure 5a. The mere existence of screw dislocations is not sufficient for dislocation-driven nanowire growth.

The formation of "pine tree" morphology further demands the simultaneous operation of both dislocation-driven growth of trunk nanowires and the VLS growth of epitaxial branch nanowires. Therefore, there must be sufficient overlap between the dislocation growth regime and the special VLS-mediated layer-by-layer growth regime. This also requires the fine control of supersaturation and the presence of hydrogen in the reactions. The total absence of hydrogen could inhibit the creation of elemental lead catalysts, a necessary first step for VLS growth of a branch nanowire. Continuous VLS growth of branches, which likely requires supersaturation higher than that of the dislocation-driven trunk, is also stopped when hydrogen is removed. Despite the cessation of growth, the growth fronts of the trunks and the branches are still "alive" and can resume growth when supply of H_2S returns, as discussed in section 2.3 and shown in Figure 6. From the theories on dislocation-driven and VLS growth, a dislocation-driven growth front can self-perpetuate indefinitely as long as the growth spiral exists, while the liquid−solid growth front in VLS can be terminated if the liquid catalyst is somehow removed, such as by evaporation, excessive wetting (coating the nanowire), or consumption. This was seen in the "brush-like" PbS pine trees whose branches reach a maximum length as we previously reported (in Supporting Information).[21] This difference is also demonstrated in the pressure-modulated tree growth (Figure 9), as retaining the catalyst droplets in VLS growth depends much more sensitively on the total pressure than the preservation of growth spiral in dislocation-driven growth. Since dislocation-driven and VLS growth are governed by different factors, it is plausible that in the future they could be separately controlled to allow further tuning of the hierarchical nanowire structures.

The discussion above puts VLS and dislocation-driven nanowire growth in competition with each other. However, VLS mechanism could also be related to dislocated nanowires. It is sometimes observed that trees with Eshelby twist can seemingly "grow out of" hyperbranched clusters with no twist (Figure 12a), which might suggest that a nanowire that is originally formed by VLS may grow for some time and then a screw dislocation is somehow introduced to the growth front. Once a dislocation is introduced, the dislocation spiral steps become the primary driving force for crystal growth, even in the presence of the catalyst. This speculation might be further strengthened by the (rare) occurrence of free-standing double-headed trees that grow in both directions (Figure 12b). Dislocations and other defects can be introduced into a crystal precipitating out of a solution if supersaturation is rapidly increased. The same idea may be applicable to nanowires precipitating out of the solution of a liquid VLS catalyst droplet since VLS is still a layer-by-layer growth after all.

4. Summary and Perspectives

In summary, we have systematically analyzed the growth of dislocation-driven PbS nanowires. The optimum conditions for synthesizing PbS nanowire pine trees have been investigated with detailed studies of morphology changes under various hydrogen, temperature, pressure, and substrate conditions. Onset of hydrogen flow at the appropriate level plus the presence of

(41) Amelinckx, S. Dislocations in alkali halide whiskers. In *Growth and Perfection of Crystals*; Doremus, R. H., Roberts, B. W., Turnbull, D., Eds.; Wiley: New York1958; pp 139−153.

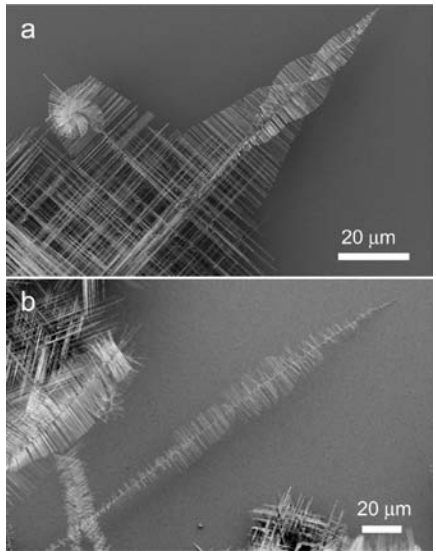

Figure 12. Possible evidence of VLS processes being involved in formation of dislocated trunk nanowires in PbS trees. (a) Rotating trees emerging from hyperbranched nanowires grown via VLS mechanism. (b) A free-standing tree that grows simultaneously in opposite directions. The dislocated trunk is expected to originate at its midpoint.

fresh silicon have been identified as the critical ingredients for generating PbS nanowire trees reproducibly in this specific reaction system. Thermodynamic considerations suggest that the actual reaction that produces PbS is between $PbCl_2$ and H_2S. Controlling and modulating the supersaturation of the reaction precursors is critical to dislocation-driven nanowire growth. The onset of hydrogen flow likely creates a spike in H_2S supersaturation and initiates dislocations with screw components that then propagate anisotropically to form the nanowire trunks. Maintaining an optimum hydrogen flow can provide a favorable supersaturation that promotes dislocation-driven trunk nanowire growth and enable the simultaneous growth of the VLS-driven nanowire branch. Furthermore, we show that silicon fortuitously controls (buffers) the supersaturation by reacting with H_2S to form SiS_2 and SiS_2 can be a viable precursor for synthesizing PbS nanowires.

In a more general context, the successful growth of nanowires driven by screw dislocations requires two basic ingredients: the creation (seeding) of dislocations and a suitably low supersaturation condition for promoting dislocation-driven growth over layer-by-layer growth and other growth modes. In the specific case of PbS trees, the generation of dislocations is spontaneous and likely due to an initial burst of high supersaturation triggered by the onset of hydrogen flow. We can imagine some intentional control over this process by "engineering" screw dislocations on the substrates. To ensure that dislocation-driven nanowire growth dominates over (or at least is not overwhelmed by) other competing growth mechanisms, a low supersaturation level needs to be maintained. In this case this is satisfied by a continuous flow of hydrogen and a fortuitous SiS_2 side reaction that dictates the H_2S concentration. This requirement can be more deliberately controlled in more rationally designed dislocation-driven nanowire growth using more sophisticated reactors in the future, such as with controlled delivery and accurate monitoring of precursor gases and multizone heating with precisely controlled temperature. Silicon (and its reaction with H_2S), as seen in the specific case of PbS nanowire growth herein, is not a necessary requirement to satisfy the conditions for dislocation-driven growth, yet this system can be conveniently implemented in a simple CVD setup, despite the intricate chemical mechanisms at work (that naturally control the supersaturation). Using H_2S gas directly as the CVD precursor could be a fruitful direction to explore; however, safety considerations regarding the toxicity of H_2S has prevented us from implementing such experiments so far. The formation of pine tree nanowires further demands a simultaneous VLS growth process to produce the branches, which means that the conditions can allow the continuous generation of VLS catalysts and maintain a supersaturation level still suitable for reasonable VLS nanowire growth. Dislocation-driven nanowire growth is a general nanowire mechanism that has been greatly under appreciated in modern literature and may manifest itself in many other materials systems prone to having screw dislocations, such as GaN[42,43] and SiC. It is very likely that by following the general understanding discussed herein, dislocation-driven nanowire growth, and possibly even "pine-tree-like" nanowire growth, can be achieved in other material systems, especially similar IV−VI and II−VI materials.

Herein, we have attempted to outline an empirical understanding of the dislocation-driven nanowire growth as exemplified by the CVD growth of PbS nanowire pine trees. However, many more specific questions regarding the PbS pine tree nanostructures and fundamental questions about dislocation-driven growth remain unanswered. For example, why is the spacing of the branches regular and the arrangement of the epitaxial branches around the trunk ordered? Why do the branches appear to always emerge following the advance of the trunk, as opposed to happening randomly on existing trunks? Are there some correlations or mutual influence between the presumed dislocation-driven trunk growth and VLS branch growth? For the future, further understanding of the dislocation-driven nanowire growth, hopefully at the more quantitative level, calls for more intentional and careful control of various reaction conditions, supersaturation being the most important. Such controls can be realized using more elaborate reactor design with precisely controlled precursor delivery, temperature, and pressure, molecular beam epitaxy perhaps being the most extreme. A fundamental understanding, possibly at the atomic level, will also benefit from in situ monitoring and observation of the nanowire growth using emerging in situ electron microscopy techniques,[44] which provides the possibility of observing the step flow and propagation of crystal growth.[45,46] Theoretical modeling and/or simulation of the nanowire crystal spiral growth can also be very useful to advance our fundamental understanding of this intriguing nanowire growth.

5. Experimental Section

Typical Synthesis of PbS Nanowire Pine Trees. General "standard" procedures for synthesizing PbS trees are presented herein. Note that this is slightly different from what we reported previously,[21] but the difference in the procedures and the products is very small. Depending on the purposes of the reactions, many experiments (>400 runs) were carried out by following this standard

(42) Jacobs, B. W.; Crimp, M. A.; McElroy, K.; Ayres, V. M. *Nano Lett.* **2008**, *8*, 4353–4358.
(43) Cherns, D.; Meshi, L.; Griffiths, I.; Khongphetsak, S.; Novikov, S. V.; Farley, N. R. S.; Campion, R. P.; Foxon, C. T. *Appl. Phys. Lett.* **2008**, *93*, 111911.
(44) Ross, F. M. *Mater. Today* **2006**, *9*, 54–55.
(45) Hofmann, S.; Sharma, R.; Wirth, C. T.; Cervantes-Sodi, F.; Ducati, C.; Kasama, T.; Dunin-Borkowski, R. E.; Drucker, J.; Bennett, P.; Robertson, J. *Nat. Mater.* **2008**, *7*, 372–375.
(46) Qiu, S. R.; Orme, C. A. *Chem. Rev.* **2008**, *108*, 4784–4822.

procedure or by varying one or a few components of these reactions as specifically discussed in the Results.

PbS nanowires were synthesized in a home-built CVD reactor consisting of pressure and multiple-gas flow controls, a 2.54 cm (outer diameter) fused silica tube placed in a single-zone tube furnace (Lindberg\Blue M), a dry ice/acetone trap, and a mechanical vacuum pump. A 25 mg portion of $PbCl_2$ in an alumina boat was placed in the tube at the center of the furnace where temperature can be exactly controlled. A freshly cleaved strip (about 5 mm × 20 mm) of silicon (100) substrate covered by 100 nm thermal SiO_2 was first cleaned using oxygen plasma and then loaded into the tube 1−2 cm downstream from the $PbCl_2$ boat. Sulfur (35 mg) in another alumina boat was placed upstream just outside the furnace. The tube was sealed and evacuated to about 10 mTorr and flushed 3 times with argon. It was then heated to 600 °C under a flow of argon at 150 standard cubic centimeters per minute (sccm), and the system pressure was maintained at 900 Torr using manometer and pressure controller. When the target temperature was reached, the sulfur boat was pushed using magnets halfway into the furnace ceramic insulation where sulfur would start to melt and hydrogen flow at 1.0−2.5 sccm was started. Reaction was typically terminated after 15 min by switching off gas flows and furnace, evacuating the tube and allowing the furnace to cool down with the lid open.

Instrumentation and Methods. The as-synthesized PbS pine tree nanostructures on silicon substrates were inspected under scanning electron microscopy (SEM) using a LEO 1530 FESEM and optical microscopy using an Olympus BX51M optical microscope with 10× eyepieces and 10×, 20×, 50×, and 100× objectives. Scale bars for the images were calibrated. Powder X-ray diffraction (PXRD) was performed on a Siemens Stoe X-ray diffractometer with a Cu Kα source.

The survey of trees that yielded the raw data for Figures 3, 4, 6, and 8 was carried out by taking a large number of SEM and optical images on multiple samples from several batches of reactions. To determine the tree length accurately, only trees with rotating branches (Eshelby twist) that lie almost horizontally to the substrate surface were measured. The error due to inclination of trees is fairly small, as a tree inclined at 30° is expected to give an error of about 15% in length. Any trees for which a large portion is obviously embedded within a dense mesh of other nanowires were also avoided in measurements because the view was obstructed. Similar rules were followed in statistical measurements of cone angles. In addition, branches from long trees sometimes seem to reach a growth limit (due to evaporation of catalyst in prolonged reactions) and give rise to a "brush" shape in the lower portion of the tree (discussed in the Supporting Information of our previous report[21]). In this situation, only the upper portion that exhibits a cone shape was used for cone angle measurement.

Acknowledgment. This research was supported by NSF (CAREER DMR-0548232). S.J. thanks the Sloan Research Fellowship, Research Corporation Cottrell Scholar Award, Exxon Mobil Solid State Chemistry Fellowship, and DuPont Young Professor Grant for support. M.J.B. thanks the support of an Air Products Fellowship. We thank M. Lukowski for experimental assistance and M. Lukowski and S. A. Morin for helpful discussions.

Note Added after ASAP Publication. The next-to-last paragraph of the Summary and Perspectives was corrected. This paper was published originally October 21, 2009; the corrected version was published October 28, 2009.

Supporting Information Available: Table of the thermodynamic free energy of formation for various chemical species and the powder X-ray diffraction pattern of the deposit containing SiS_2. This material is available free of charge via the Internet at http://pubs.acs.org.

JA906499A